PHYSICAL REVIEW B VOLUME 25, NUMBER 4 15 FEBRUARY 1982

Vibronic spectra of Gd^{3+} in metaphosphate glasses: Comparison with Raman and infrared spectra

D. W. Hall, S. A. Brawer, and M. J. Weber
Lawrence Livermore National Laboratory, University of California, Livermore, California 94550
(Received 13 August 1981)

Vibronic sidebands associated with the $^6P_{7/2} \rightarrow {}^8S_{7/2}$ transition of Gd^{3+}-doped metaphosphate glasses are observed using line-narrowed fluorescence techniques. Glasses having metal cations of different mass and charge (La,Al,Mg,Ba) are examined. Vibronic spectra, which probe vibrations about the rare-earth element site, are compared with polarized Raman scattering data and the infrared dielectric constant obtained from near-normal reflectance measurements. Results indicate that in metaphosphate glasses vibronic selection rules are similar to *HV* Raman selection rules. The wavelengths and relative intensities of peaks in the high-frequency portion of the vibronic spectra change with respect to corresponding peaks in the Raman spectra when the mass and/or charge of Gd^{3+} differs significantly from that of the metal cation.

I. INTRODUCTION

Vibronic sidebands arise from combined electronic-vibrational transitions of optically active ions in solids. They are commonly observed in optical spectra and, in several cases, are well understood.[1] Vibronic spectra provide a valuable probe for investigating the strength of the electron-phonon coupling and the nature of vibrations about an ion site. The localized character of vibronic spectroscopy complements other spectroscopies, such as infrared absorption, Raman scattering, and neutron scattering, which generally measure intrinsic vibrational properties of the solid.

Studies of vibronic transitions in glass are complicated by the disordered nature of the host. This disorder causes inhomogeneous broadening of spectral features due to the distribution of perturbing environments experienced by ions in glass. Purely electronic, zero-phonon transitions of different classes of ion sites occur at different frequencies. In addition, site-to-site differences in the field stength and local vibrational modes are expected to affect the frequency and intensity of associated vibronic transitions.[2] For nonselective excitation, these spectra are superimposed into a broad, unresolved spectrum.

The only previously reported observations of vibronic sidebands in glass[3,4] employed a rare-earth element (Eu^{3+}) as the probe ion. Trivalent europium has a relatively simple energy-level scheme and, for $4f$-$4f$ transitions, the ion-phonon coupling is weak. Vibronic transitions were detected in the $^7F_0 \rightarrow {}^5D_0$ excitation spectrum of the strong $^5D_0 \rightarrow {}^7F_2$ emission. Zakharov *et al.*[3] found that they could correlate many of the observed vibronic bands with bands in the infrared reflection spectra, but in a number of cases, vibronic frequencies could not be correlated with any infrared frequency. In these nonresonant studies, the vibronic spectra were subject to the same inhomogeneous broadening as the zero-phonon line.

Selective excitation of ions with similar local environments in glass is possible using techniques of laser-induced fluorescence line narrowing.[2] By using a tunable excitation source, site-to-site variations in energy levels and transition probabilities have been measured. We have used this technique to circumvent inhomogeneous broadening and reveal true vibronic band widths. By emphasizing the frequency difference between the fluorescence sidebands and the center of the line-narrowed zero-phonon line, we map out the density of states of vibrations around a single subset of fluorescing ion, weighted by vibronic selection rules.

Trivalent gadolinium as a dilute impurity was selected for the probe ion. This ion is well suited for vibronic studies because its ground level is an S state which experiences negligible splitting in any perturbing environment. Thus there is no confusion from overlapping vibronic transitions and zero-phonon transitions to different Stark levels of the terminal J-state manifold. In addition, there are no other J states within a single phonon energy

of the terminal state to obscure the weak vibronic signal.

Metaphosphate glasses were chosen for the host because their structure has been studied and portions of their vibrational spectra have been characterized in terms of the motions of simple structural units.[5-7] This characterization is not rigorously established, however. Metaphosphate glasses have the stoichiometry $M(PO_3)_x$, where M represents a metal modifier cation and x is the oxidation state of the metal. Their structure is considered to be basically the same regardless of M and consists of PO_4 tetrahedron connected at two corners forming polymeric chains. Modifier cations and rare-earth (RE) dopants occupy sites between nonbridging oxygen atoms and provide weak linkage between different chains.

As metal modifier cations we chose (1) La^{3+}, an ion similar to Gd^{3+} in mass and charge, and (2) Al^{3+}, Ba^{2+}, Mg^{2+} ions which differed from Gd^{3+} in mass and/or charge. Thus we studied cases where the RE probe ion constituted a negligible perturbation as well as cases where it was both a mass and a charge defect.

To obtain information about the vibrations of the unperturbed glass, polarized Raman scattering spectra and near-normal infrared reflectance spectra were recorded for all of the glasses. These traditional vibrational spectroscopies obey different selection rules and thereby emphasize different vibrational modes. For the low RE concentrations in our samples, the vibrational spectra are characteristic of the undoped bulk glass. Because of dispersion associated with infrared reflection, the quantity most indicative of ir-active vibrational modes is the imaginary part of the dielectric constant ϵ_2. This was obtained numerically from reflectance data using a Kramers-Kronig transformation.

Goals of this investigation were (1) to discover if vibronic spectra are representative of vibrations of the entire glass network or of impurity modes created by the presence of the RE, and (2) to determine the selection rules for coupling of vibronic transitions to different vibrational modes. Similar studies of a beryllium fluoride glass in which a search was made for site-to-site variations in the vibronic spectrum will be presented elsewhere.

II. EXPERIMENTAL

Samples

The following metaphosphate glasses were investigated (compositions in mol %):

$50P_2O_5 \cdot 49MO \cdot 1Gd_2O_3$, where $M = Mg, Ba$

and

$75P_2O_5 \cdot 24M_2O_3 \cdot 1Gd_2O_3$, where $M = Al, La$.

Samples were prepared by the Inorganic Glass Section of the National Bureau of Standards from reagent-grade materials using normal melting and casting methods. Typical size of polished samples was $10 \times 10 \times 5$ mm^3.

Fluorescence line narrowing

Gadolinium ions were excited into the $^6P_{7/2}$ band with a frequency-doubled, pulsed rhodamine 6G dye laser (Chromatix CMX-4). The spectral width and pulse duration were <3 cm^{-1} and ~ 1 μs, respectively. Samples were mounted in a Dewar and cooled to $\simeq 20$ K using a closed-cycle He refrigerator. A right-angle excitation-observation geometry was used. Fluorescence spectra were observed using a 1-m grating monochromator, an ambient-temperature S-20 phototube (Amperex PM2233A), and gated photon-counting electronics. A polarization scrambler was placed between the sample and entrance slit of the monochromator. The spectrometer was controlled by an an LSI-11 computer that allowed averaging of several experimental runs. A reference channel and normalization procedures were used to account for variations in laser pulse energy. Resolution of the apparatus was slitwidth limited and <30 cm^{-1}; the spectral accuracy was $\simeq 5$ cm^{-1}.

To obtain true vibronic peak widths, line narrowing must be complete. If not, vibronic spectra are a convolution of shifted sidebands due to ions in different environments. Since the homogeneous linewidth of purely electronic transitions of RE's in glass has been observed[8] to vary as T^2, site selectively and line narrowing are enhanced at low temperatures. This is illustrated in Fig. 1. Low sample temperatures also simplify spectra because only the lowest energy state of the excited $^6P_{7/2}$ manifold will be populated. In addition, for optimal line narrowing, excitation should be limited to the low-frequency tail of the inhomogeneously broadened $^8S_{7/2} \rightarrow {}^6P_{7/2}$ absorption band. This reduces the possibility of accidental coincidences of excitation bands. An accidental coincidence occurs, for example, when the lowest energy level of the $^6P_{7/2}$ manifold of one ion is equal in energy to another $^6P_{7/2}$ level of an ion in a different local environment. The same excitation frequency re-

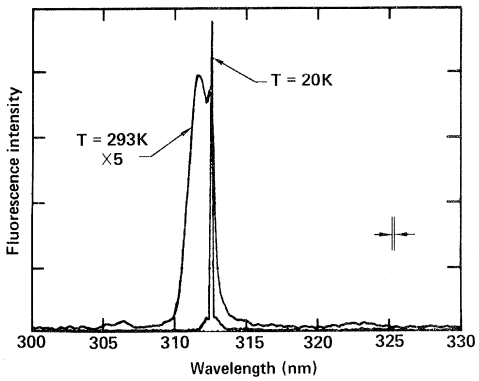

FIG. 1. Laser-excited $^6P_{7/2} \rightarrow {}^8S_{7/2}$ fluorescence of Gd^{3+} in $Ba(PO_3)_2$ glass. Excitation wavelength: 312.5 nm.

sults in resonant and nonresonant zero-phonon fluorescence transitions of different energies and therefore a superposition of vibronic side bands.

Fluorescence lifetimes of the $^6P_{7/2}$ state of Gd^{3+} in the different metaphosphate glasses ranged from 3–5 ms. Since scattered incident laser light was insignificant, a photon counting gate of 5 ms beginning at $t=0$ could be used. To test for cross relaxation (energy transfer between different RE sites), we compared line-narrowed zero-phonon spectra recorded at zero delay and at 7-ms delay using a 1-ms gate. No detectable changes in spectra shape were observed, indicating that at doping levels of 1 mol %, negligible cross-relaxation occurred within the 5-ms gate duration used in recording vibronic spectra.

Raman spectra

Raman spectra were obtained at room temperature using either the 488.0- or the 514.5-nm line of a Spectra Physics argon ion laser (model 165). A 90° scattering geometry was employed incorporating polarizer, polarization scrambler, and a SPEX model 1401 double monochromator as analyzer. The detection system consisted of a cooled RCA 31034A phototube in a photon-counting mode. Counting rates were typically 5×10^4 s^{-1}. Raman spectra were not corrected for population of low-frequency phonon modes at room temperature. Resolution of the apparatus was <5 cm^{-1}.

Infrared spectra

Infrared reflectance was measured at 15° from normal using a DIGILAB FTS14 Fourier transform spectrometer. Data from 170–400 cm^{-1} were recorded using a Mylar beam splitter and from 400–4000 cm^{-1} using Ge on KBr. A front-surface gold mirror was used as reference and assumed to be 100% reflecting in the region of measurement.

III. RESULTS

Laser-excited resonant $^6P_{7/2} \rightarrow {}^8S_{7/2}$ fluorescence of $Ba(PO_3)_2$:Gd^{3+} at 293 and 20 K is shown in Fig. 1. At low temperatures the homogeneous linewidth is reduced, which greatly improves the line narrowing and increases the site selectivity. At 293 K, weak Stokes-shifted vibronic sidebands are observed extending out to $\simeq$ 325 nm. The peak vibronic amplitude is only 1/50th the magnitude of the zero-phonon line. A search was made for two-phonon vibronic sidebands but none were detected; this placed an upper limit on their intensity of $<10^{-3}$ of the zero-phonon intensity. The weak fluorescence band in Fig. 1 at $\simeq$ 307 nm is $^6P_{5/2} \rightarrow {}^8S_{7/2}$ emission.

The infrared reflectance of $La(PO_3)_3$:Gd glass is shown in Fig. 2. The structure in this spectrum is typical of that observed for all of our glasses.

Vibronic spectra for the metaphosphate glass series are shown in Figs. 3–6. The abscissa represents the frequency shift of the phonon-assisted fluorescence from the peak of the line-narrowed zero-phonon line. The large increase in the vibronic intensity at low frequency does not imply a large density of states but is the result of a

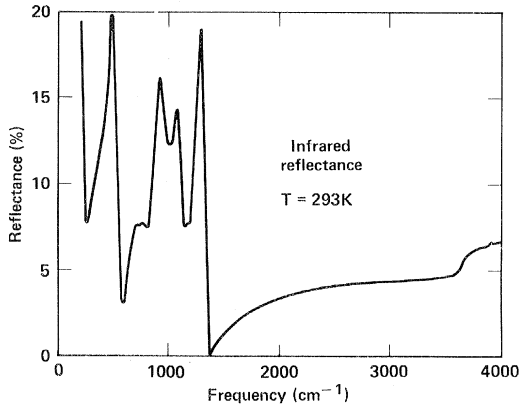

FIG. 2. Infrared reflectance spectrum of $La(PO_3)_3$:Gd glass recorded at 15° from normal.

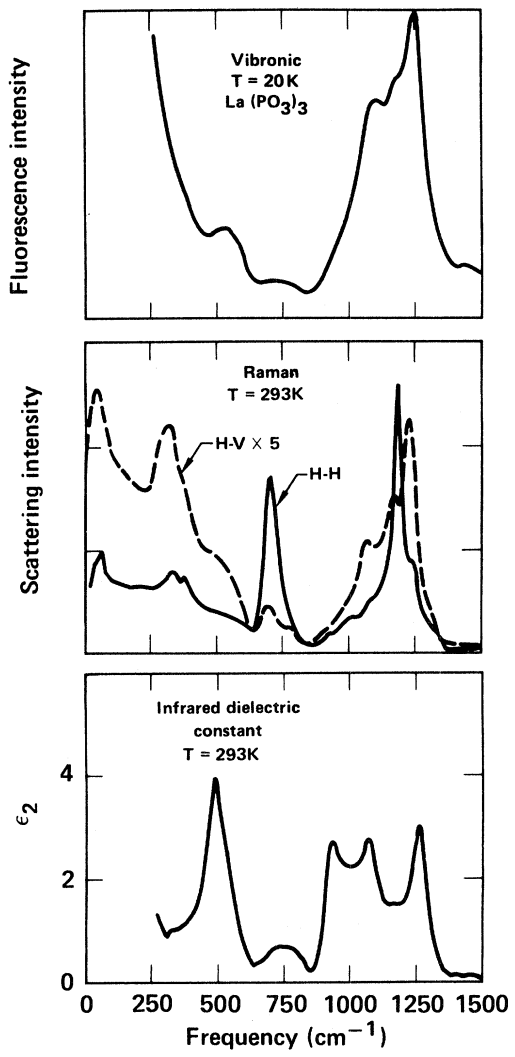

FIG. 3. Comparison of the vibronic, *HH* and *HV* polarized Raman, and infrared (dielectric constant) spectra of $La(PO_3)_3$:Gd glass.

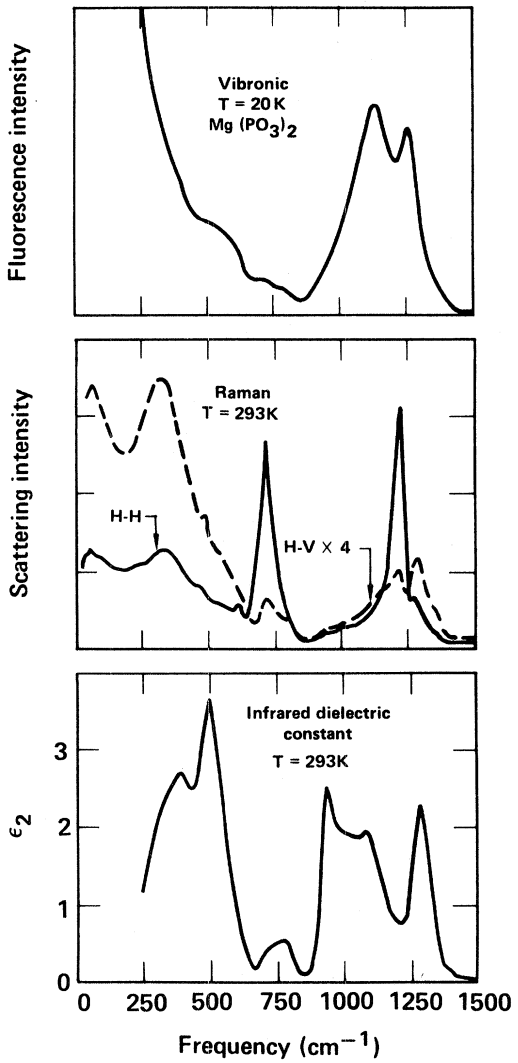

FIG. 4. Comparison of the vibronic, *HH* and *HV* polarized Raman, and infrared (dielectric constant) spectra of $Mg(PO_3)_2$:Gd glass.

superposition of vibronic signal and the tail of the intense zero-phonon line (observed with a spectral slitwidth of 30 cm^{-1}).

Also plotted in Figs. 3—6 are *HH* and *HV* Raman spectra. The notations *HH* and *HV* indicate spectra recorded with the polarization of the incident and scattered radiation parallel or perpendicular to one another, respectively.

The infrared dielectric constant ϵ_2 was obtained from the ir reflectance spectrum and is also included in Figs. 3—6. It was derived from a Kramers-Kronig transform performed using trapezoidal-rule integration on a PDP-11/40 minicomputer. No significant change in optical constants occurred above 250 cm^{-1} when widely varying reflectances were substituted for the unmeasured low-frequency region (< 170 cm^{-1}). Reflectance in the unmeasured high-frequency region (> 4000 cm^{-1}) was assumed constant and equal to the value at 4000 cm^{-1}. Optical constants in the range 250—1500 cm^{-1} were insensitive to other values and boundary conditions.

Frequencies of prominent features in vibronic, Raman, and infrared spectra are tabulated in Table I. Comparison of the high-frequency peaks from the RE-doped samples and from the undoped unpolarized data of Nelson and Exarhos[7] confirms that Raman scattering, which probes regions of spatial scale $> 3—4$ nm, is not affected by the small addition of RE.[9]

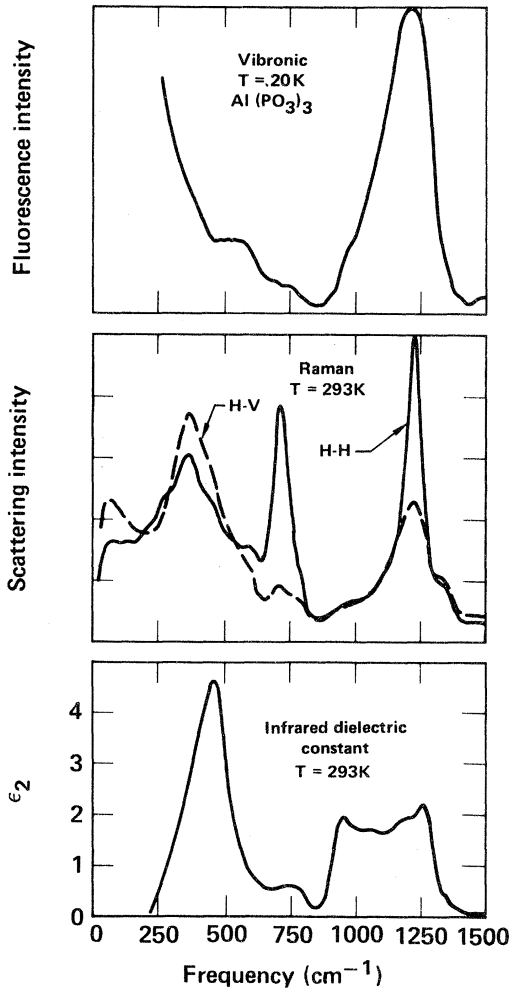

FIG. 5. Comparison of the vibronic, *HH* and *HV* polarized Raman, and infrared (dielectric constant) spectra of $Al(PO_3)_3$:Gd glass.

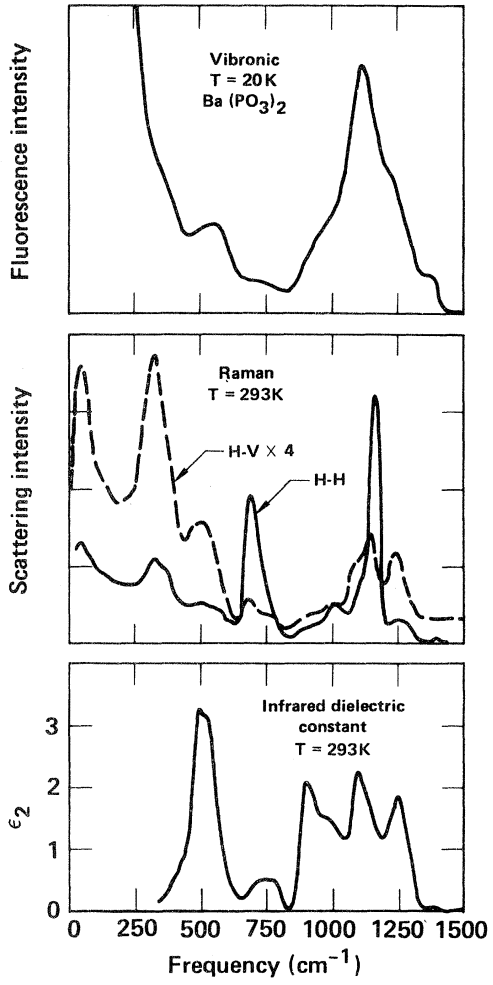

FIG. 6. Comparison of the vibronic, *HH* and *HV* polarized Raman, and infrared (dielectric constant) spectra of $Ba(PO_3)_2$:Gd glass.

IV. DISCUSSION

Before discussing the vibronic spectra, we review the Raman and infrared spectra of the various metaphosphate glasses. Vibronic, Raman, and infrared spectra are strongly governed by selection rules.[9] Because these rules are different for each spectroscopy, the relative intensities of peaks in the various spectra are not identical. The relationship of these spectra to the vibrational density of states depends on the selection rules and coupling strength.[10,11] Since these depend on the nature of the vibrational modes, neither the vibronic, Raman, nor infrared spectrum provides a direct measure of the density of states.

Raman spectra

Raman scattering spectra emphasize those vibrational modes with a displacement-dependent polarizability. Spectra of all of our metaphosphate glasses are qualitatively the same, reflecting the similarity of their basic structure regardless of the metal cation. The most prominent bands observed in the *HH* and *HV* polarizations occur in the vicinity of 50, 330, 700, and 1200 cm^{-1}; the exact location of peaks are given in Table I.

It is clear that the *HH* and *HV* spectra obey different selection rules. The two highest-frequency bands exhibit structure and a strong polarization dependence, whereas the lower-frequency bands do not. The *HV* spectra contain all features of the

TABLE I. Comparison of peak frequencies observed in *HV* Raman (T=293 K), infrared (T=293 K), and Gd^{3+} vibronic (T= 20 K) spectra for various metaphosphate glasses. Typical uncertainties in determining the peak positions are indicated. All frequencies are in cm^{-1}.

Glass	$Mg(PO_3)_2$	$Al(PO_3)_3$	$Ba(PO_3)_2$	$La(PO_3)_3$
HV Raman:				
*R*1	1272±5	1331	1249	1232
*R*2	1210±5	1225	1152	1177
Ref. 7	1210	1220	1163	1181
*R*3	1130±15		1095	1080
*R*4	803±10	788	771	784
*R*5	707±5	715	689	696
*R*6			495	500
*R*7	329	355	333	333
Infrared:				
*I*1	1283±10	1259	1250	1259
*I*2	1085±10		1100	1066
*I*3	926±10	950	907	926
*I*4	750±20	750	750	750
*I*5	482±10	458	500	482
*I*6	380	400		
Ref. 7	405	400	143	189
Vibronic:				
*V*1	1245±15	1210	1225	1235
*V*2				1170±15
*V*3	1120±15		1110	1095
*V*4	710±30	750	725	750
*V*5	530±30	550	550	530

HH spectra (with different relative intensities) plus several additional peaks. These latter peaks are not resolved in previously reported *unpolarized* spectra,[5–7] although there are hints of shoulders in these data.

The widths of the Raman lines are comparable for all glasses except for $Al(PO_3)_3$. The broader features in the latter glass are attributed to the ability of Al to be incorporated as both a glass network former and network modifier which introduces disorder and relaxes selection rules. The presence of Al in other oxide glasses also results in the broadening of spectral features.[12]

The high-frequency vibrational bands in metaphosphate glasses have been associated with motions within the phosphate chain with mode frequencies slightly perturbed by the modifier cations. Assignments of these (unpolarized) bands have been made by Bobovich.[5] The band at ~700 cm^{-1} (*R*5) was assigned to P—O—P stretching modes of the chain itself. The highest frequency band at ~1200 cm^{-1} was assigned to motion of the two nonbridging oxygens per tetrahedron (PO_2 group) relative to the phosphorus-bridging oxygen polymeric chain. Specifically, the dominant high-frequency peak in the unpolarized Raman spectra (which is equivalent to the large *HH* peak at frequency labeled *R*2 in Table I) is assumed due to a PO_2 symmetric stretch while a satellite at slightly higher frequency (*R*1) is assigned to a PO_2 asymmetric stretch.

The frequencies of the two peaks *R*1 and *R*2 vary systematically with metal cation (see Table I). Rouse *et al.*[6] have explained the shift of the highest-frequency vibration band in diffrent alkali metaphosphate glasses using a simple, four-particle vibrational model. In this model, mode frequencies depend on the metal-nonbridging oxygen force constant and the PO_2 bond angle, both of which are governed primarily by metal cation size. They were successful in predicting a linear decrease of peak frequency with increasing cation size and differnt rates of change of the symmetric and asymmetric mode frequencies. Their model, however, does not contain enough degrees of freedom to explain all the high-frequency features of *polarized*

Raman spectra. One example is the peak labeled $R3$, which is clearly resolvable in $La(PO_3)_3$ and appears as a definite shoulder in the other materials. This peak does not vary consistently with cation size.

Infrared spectra

The ϵ_2 spectra for all of the metaphosphate glasses in Figs. 3–6 are qualitatively similar, demonstrating again the commonality of their basic structures. Again, the $Al(PO_3)_3$ glass has broader features with no resolved structure in the highest-frequency band. Although the broad bands in the ϵ_2 spectra at ~ 500 and 750 cm^{-1} show general correspondence with bands in the Raman spectra, high-frequency peaks such as $I3$ show no correspondence with strong peaks in either the Raman or vibronic spectra. The peak $I6$ arises from the vibration of the metal cation in its cage of surrounding oxygens. The frequency of this cation motion has been studied in a series of metaphosphate glasses using far-infrared absorption data[7] and is included in Table I. A well-resolved peak corresponding to this mode is observed in the ϵ_2 spectrum of $Mg(PO_3)_2$ glass and a shoulder is observed for the $Al(PO_3)_3$ glass; for the other glasses the frequency of this mode is below our range of observation.

Infrared experiments probe those vibrational modes that create a macroscopic electric-dipole moment. The nature of the infrared-active vibrational modes in glass have been discussed by Galeener and Lucovsky.[13] These authors claim that peaks in the ϵ_2 spectrum are associated with vibrations having transverse-optical-mode character whereas peaks in the energy-loss function, $-\mathrm{Im}(1/\epsilon)$, are associated with vibrations having longitudinal-optical-mode character. They also report evidence of a longitudinal-optic–transverse-optic (LO-TO) splitting in the polarized Raman spectra of GeO_2, SiO_2, and BeF_2 analogous to that found in crystals.[13,14] The definitive experiment to verify a LO-TO splitting in glass has not been performed.

It is not at all clear whether in fact the above concepts of transverse and longitudinal character apply to glasses. In these materials, most modes are probably localized and high-frequency vibrations might more reasonably resemble a set of independent, nearly uncoupled oscillators. In particular, because of the inhomogeneous broadening of ϵ_2 arising from the presence of vibrating entities with different frequencies, the function $-\mathrm{Im}(1/\epsilon)$ does not represent the "longitudinal" vibrations of such entities. We have calculated the energy-loss function from the ir reflectance spectra. The loss function of $La(PO_3)_3$:Gd glass is shown in Fig. 7 and is typical of that obtained for all our glasses. Peaks in $-\mathrm{Im}(1/\epsilon)$ do not correspond with strong peaks in the vibronic, Raman, or ϵ_2 spectra for any of the four metaphosphate glasses.

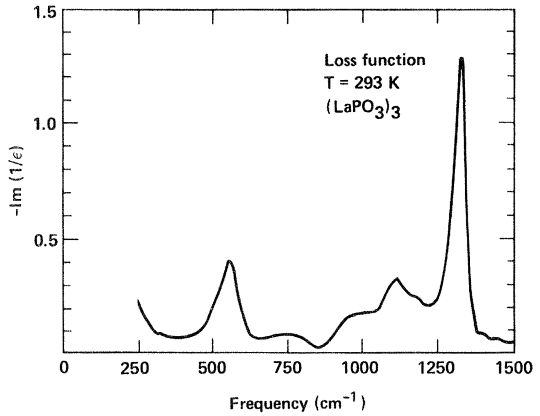

FIG. 7. Energy-loss function of $La(PO_3)_3$:Gd glass.

It is well established that the short-range order in inorganic glasses and crystals with similar compositions (if they exist) is very similar. Also, for silicates, phosphates, and borates, similar vibrational selection rules are observed in glass and crystal. In both glass and crystal, vibrational modes which are strongly Raman active are also strongly polarized and nearly infrared inactive. Conversely, modes which are weakly Raman active tend to be depolarized and hence appear in the HV spectrum. The depolarized modes are often the ones that are strongly infrared active. This does not appear to be satisfied for metaphosphate glasses, because the ϵ_2 spectra are quite different from the HV Raman spectra.

Vibronic spectra

Vibronic transitions involve an electronic transition accompanied by the creation-annihilation of phonons. Thus they probe those vibrations which create a displacement-dependent electric field at the RE site. This dynamic crystal field is a microscopic quantity in contrast to the macroscopic field involved in Raman and ir experiments. For simple crystals possessing tetrahedral symmetry, the macroscopic and microscopic electric fields are simply related.[15] For less symmetric crystals the relationship is complex. For impurity sites in glass

the relationship is not clear.

The vibronic spectra of Gd^{3+} in metaphosphate glasses are similar to the Raman and ir spectra insofar as general bands are again observed in the vicinity of 500, 750, and 1200 cm^{-1}. As noted earlier, lower frequency modes are obscured by the tail of the zero-phonon line. Potentially intense modes involving motion of the RE dopant with respect to its neighboring oxygens are expected to occur at < 200 cm^{-1} and hence are unresolved in our experiments. This estimate is based on far-infrared (fir) absorption measurements[7] of $Gd(PO_3)_3$ glass where the cation motion band is centered at 195 cm^{-1}. Low-frequency vibrations associated with the metal cation occur at 143, 189, 405, and > 400 cm^{-1} in the fir spectra of Ba, La, Mg, and Al metaphosphate glasses, respectively. These bands would be partially or fully obscured in our vibronic spectra.

The most striking result of a comparison of the different spectroscopies, apparent from Figs. 3–6, is the similarity of the high-frequency *HV* Raman and vibronic spectra. This is especially true for $La(PO_3)_3$ glass, which is shown in greater detail in Fig. 8. In this material the RE (Gd) is most like the network modifying cation (La) — the ionic charges are the same and the masses differ by only 12%. The locations of the *R*1, *R*2, *R*3, and *V*1, *V*2, *V*3 peaks match within the spectral accuracy of our experiment; the relative intensities of the peaks are also nearly the same. This correspondence implies that for metaphosphate glasses, vibronic selection rules are similar to those of *HV* Raman scattering.

In the $Mg(PO_3)_2$ glass, the RE is both a mass and a charge defect. Still, there is a twin-peaked

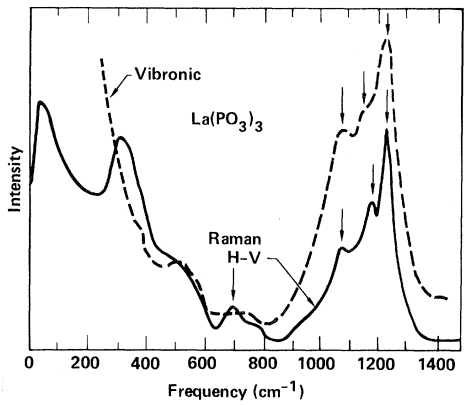

FIG. 8. Detailed comparison of the vibronic and *HV* Raman spectra of $La(PO_3)_3$:Gd glass.

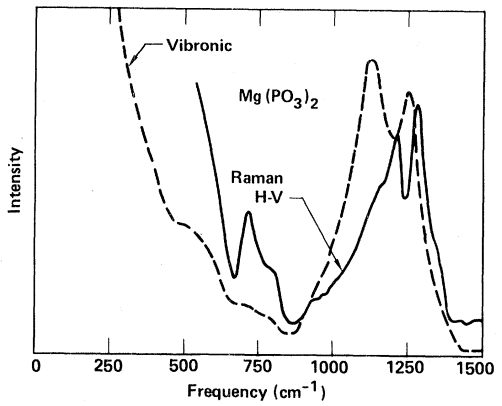

FIG. 9. Detailed comparison of the vibronic and *HV* Raman spectra of $Mg(PO_3)_2$:Gd glass.

high-frequency band in both the *HV* and vibronic spectra, but with a change in relative intensities and with the locations of the peaks in the vibronic spectrum lower by ≈ 30 cm^{-1}. This is illustrated in Fig. 9. These differences are presumably the result of the perturbing RE. However, the broad band at 750 cm^{-1} and the shoulder at ~ 530 cm^{-1} coincide in frequency with those in the Raman spectrum.

Although the highest-frequency vibronic band of the $Ba(PO_3)_2$ glass is not twin peaked, the locations of the maxima and shoulder of this band are the same as the two distinct high-frequency peaks in the *HV* Raman spectrum. The weaker bands at ~ 750 and 550 cm^{-1} are generally the same in the two spectra.

The general features of the *HV* Raman and vibronic spectra of $Al(PO_3)_3$ glass are similar, however, any correlation of peaks is obscured by the broadening of spectral features mentioned previously.

As seen in Figs. 3–6, the vibronic spectra are very different in shape from either the *HH* Raman or ϵ_2 spectra. The vibronic spectrum is completely different from the $-\mathrm{Im}(1/\epsilon)$ spectrum.

Vibronic transitions of rare-earth ions in solids are predominantly of electric-dipole nature. For $4f$-$4f$ transitions, they become allowed by admixing of states of opposite parity by the dynamic crystal field. Judd[16] has shown that the probability for one-phonon vibronic transitions of rare earths can be expressed in terms of a summation of products of phenomenological intensity parameters and matrix elements of tensor operators between states of $4f^n$. The parameters involve terms of odd-order spherical harmonics in the expansion of the dynamic crystal field. The contributions from

terms of order N decrease with separation R between the rare earth and neighboring ion as $1/R^{N+1}$. Therefore, the contributions to the third- and higher-order terms arise mainly from short-range interactions. The first-order term, however, decreases as $1/R^2$ and hence is relatively long range. For transitions between states where all terms are allowed by electric-dipole selection rules, vibrations of both ligands and more distant neighbors can, in principle, contribute to phonon-assisted transitions.

As discussed at the end of the section on infrared spectra, the *HV* Raman spectrum consists of bands which might be expected to be infrared active. These modes have an associated induced dipole moment and would contribute strongly to the first-order terms in the dynamic crystal field. They would therefore be effective in inducing vibronic transitions of rare-earth ions. This could account for the similarity of the *HV* Raman and vibronic spectra.

On the other hand, strongly polarized Raman modes in these materials are very weakly ir active, which is consistent with the differences between *HH* and vibronic spectra. However, the great difference between ϵ_2 and vibronic spectra is not consistent with these ideas.

Rationalization of the above correlations requires a detailed knowledge of the motions of ions about the rare earth and the site-to-site variations throughout the glass. Simple molecular models of the local structure, while valuable for qualitative understanding of vibrations in bulk glass, probably will not suffice. An understanding of a selection rules and ion-phonon coupling in glass on a microscopic scale is needed.

V. CONCLUSIONS

Fluorescence line-narrowed vibronic spectra of Gd^{3+} in glass provides an independent vibrational spectroscopy that differs from the more conventional spectroscopies (Raman, ir, neutron) in that it probes vibrations on a localized scale. We have found that in metaphosphate glasses:

(1) The vibronic sidebands of the Gd^{3+} $^6P_{7/2} \rightarrow {}^8S_{7/2}$ fluorescence are weak but provide a clear, unambiguous system for studies of vibrations in solids.

(2) In metaphosphate glasses, when the Gd^{3+} probe ion is similar to the glass modifier cation in mass and charge, the vibronic spectrum reflects selection rules and relative intensities comparable to those for *HV* Raman scattering.

(3) When the Gd^{3+} probe ion differs from modifier cation in charge or mass, gross features of the vibronic and *HV* Raman spectra are similar, however vibrational frequencies associated with the network former (PO_4) may be perturbed.

(4) Vibronic spectra of Gd^{3+} in metaphosphate glasses differ greatly from *HH* Raman and ϵ_2 spectra.

ACKNOWLEDGMENTS

We would like to express our appreciation to Dr. F. Milanovich for the use and operation of the Raman spectrometer and to Dr. D. Ottesen for providing the infrared reflection spectra. We are also indebted to D. H. Blackburn of the National Bureau of Standards for preparation of the metaphosphate samples. Work performed under the auspices of the Division of Materials Sciences of the Office of Basic Energy Sciences, U. S. Department of Energy, and the Lawrence Livermore National Laboratory under Contract No. W-7405-Eng-48.

[1]See, for example, W. A. Wall, Theory of Vibronic Spectra, in *Optical Properties of Ions in Solids,* edited by B. DiBartolo (Plenum, New York, 1974), p.187.

[2]M. J. Weber, in *Laser Spectroscopy of Solids,* edited by W. M. Yen and P. M. Selzer (Springer, Berlin, 1981), p.189.

[3]V. K. Zakharov, I. V. Kovaleva, V. P. Kolobkov, and L. F. Nikolaev, Opt. Spektrosk. 42, 926 (1977) [Opt. Spectros. (USSR) 42, 532 (1977)].

[4]V. P. Lebedev and A. K. Przhevuskii, Opt. Spektrosk. 48, 932 (1980) [Opt. Spectrosc. (USSR) 48, 513 (1980)].

[5]Ya. S. Bobovich, Opt. Spektrosk. 13, 492 (1962) [Opt. Spectrosc. (USSR) 13, 274 (1962)].

[6]G. B. Rouse, P. J. Miller, and W. M. Risen, J. Non-Cryst. Solids 28, 193 (1978).

[7]B. N. Nelson and G. J. Exarhos, J. Chem. Phys. 71, 2739 (1979).

[8]J. Hegarty and W. M. Yen, Phys. Rev. Lett. 43, 1126 (1979).

[9]S. A. Brawer, Phys. Rev. B 11, 3173 (1975).
[10]R. S. Shuker and R. W. Gammon, Phys. Rev. Lett. 25, 222 (1970).
[11]F. L. Galeener and P. N. Sen, Phys. Rev. B 17, 1928 (1978).
[12]S. A. Brawer and W. B. White, J. Non-Cryst. Solids 23, 261 (1977).
[13]F. L. Galeener and G. Lucovsky, and Phys. Rev. Lett. 37, 1474 (1976).
[14]F. L. Galeener, G. Lucovsky, and R. H. Geils, Solid State Commun. 25, 405 (1978).
[15]M. Born and K. Huang, *Dynamical Theory of Crystal Lattices* (Oxford University Press, London, 1954), p.101.
[16]B. R. Judd, Phys. Rev. 127, 750 (1962).